Long-term effects of increased adoption of artemisinin combination therapies in Burkina Faso

Robert J. Zupko[1*], Tran Dang Nguyen[1], Anyirékun Fabrice Somé[2], Thu Nguyen-Anh Tran[1], Jaline Gerardin[3], Patrick Dudas[4], Dang Duy Hoang Giang[5], Amy Wesolowski[6], Jean-Bosco Ouédraogo[7], Maciej F. Boni[1]

[1] Center for Infectious Disease Dynamics, Department of Biology, Pennsylvania State University, University Park, PA, USA

[2] Institut de Recherche en Sciences de la Santé, Direction Régionale de l'Ouest, Bobo Dioulasso, Burkina Faso

[3] Department of Preventive Medicine and Institute for Global Health, Northwestern University, Chicago, IL, USA

[4] Institute for Computational and Data Sciences, Pennsylvania State University, University Park, PA, USA

[5] Wellcome Trust Major Overseas Programme, Oxford University Clinical Research Unit, Hospital for Tropical Diseases, Ho Chi Minh City, Vietnam

[6] Department of Epidemiology, Johns Hopkins Bloomberg School of Public Health, Baltimore, MD, USA

[7] Institut de Recherche en Sciences de La Santé, Bobo-Dioulasso, Burkina Faso

* Corresponding Author, rbz5100@psu.edu

Date of this Draft: Aug 19, 2021

Word Count: 4865

Keywords: Anti-Malarial Drug Resistance, Artemisinin Combination Therapy, Burkina Faso, Malaria

Abstract

Artemisinin combination therapies (ACTs) are the WHO-recommended first-line therapies for uncomplicated *Plasmodium falciparum* malaria. The emergence and spread of artemisinin-resistant genotypes is a major global public health concern. To explore how the increased adoption of ACTs may affect the high-burden high-impact malaria setting of Burkina Faso, we added spatial structure to a validated individual-based stochastic model of *P. falciparum* transmission and evaluated long-term effects of increased ACT use. We explored how *de novo* emergence of artemisinin-resistant genotypes may occur under scenarios in which private-market drugs are eliminated or multiple first-line therapies (MFT) are deployed. We found that elimination of private market drugs would reduce the long-run treatment failures. An MFT policy with equal deployment of artemether-lumefantrine (AL) and dihydroartemisinin-piperaquine (DHA-PPQ) may accelerate near-term drug resistance and treatment failure rates, due to early failure and substantially reduced treatment efficacy resulting from piperaquine-resistant genotypes. A rebalanced MFT approach (90% AL, 10% DHA-PPQ) results in better long-term outcomes than using AL alone but may be difficult to implement in practice.

Introduction

Despite the United Nations' Millennium Development Goals leading to substantial reductions in the global burden of infectious disease, malaria remains a serious public health risk in many parts of Africa, Asia, and South America. *Plasmodium falciparum* malaria remains holoendemic in at least eleven countries, mainly in western and central Africa, and these countries have recently come under a WHO grouping called high-burden high-impact (HBHI) which recognizes that the most severely affected malaria-endemic countries will require additional resources and greater policy imagination (WHO 2019, p. 24). The two primary concerns in HBHI countries are high and widespread vectorial capacity and insufficient access to high-efficacy antimalarial therapies. Traditionally, drug-resistance concerns in holoendemic settings are of secondary importance because of the historical relationship between low-transmission regions and drug-resistance emergence and the relatively weak selection pressure imposed by lower levels of antimalarial use.

Artemisinin-resistant phenotypes were first identified in 2007-2008 in western Cambodia and have since been linked to a number of point mutations in the *P. falciparum kelch13* gene (Ariey et al. 2014; Ashley et al. 2014). Since the identification of these molecular markers, artemisinin resistance has been found in in Bangladesh, Guyana, Laos, Myanmar, Papua-New Guinea, Thailand, Rwanda, and Vietnam (Ashley et al. 2014; Chenet et al., 2015; Mathieu et al. 2020; Miotto et al. 2020; WHO 2019; Uwimana et al., 2020). Artemisinin-resistant parasites can either be imported from other regions (e.g., spread across Southeast Asia), or they may emerge independently as in Guyana, Papua-New Guinea, and Rwanda (Ashley et al. 2014; Chenet et al., 2015; Uwimana et al., 2020). This raises the possibility that HBHI countries may be at risk artemisinin resistance appearing due to *de novo* emergence or the importation of a resistant parasite.

Burkina Faso has been identified as an HBHI nation and malaria remains the leading cause of hospitalization in the general population (45.8% of all hospitalizations) as well as for children under five (48.2%) (WHO 2019; Ministère de la Santé 2020, p. 40). Malaria transmission is endemic throughout the country and seasonal transmission is aligned with the rainfall patterns of the three seasonal zones. The northern Sahelian region has a short-peak transmission season of approximately three months, increasing to four months in the central Sudano-Sahelian region, and reaching about five months in the southwestern Sudanian region (Ministère de la Santé 2016, p. 24). Artemisinin combination therapies have been in use in Burkina Faso since their adoption in 2005, resulting in significant reductions in malaria prevalence (Ministère de la Santé 2016, p. 28; Weiss et al. 2019; WHO 2019). Alongside increasing access to ACTs, local public health officials have also credited broader adoption of insecticide-treated mosquito nets (ITNs), higher levels of indoor residual spraying (IRS), and new programs in intermittent preventive treatment of pregnant women (IPTp) and seasonal malaria chemoprevention (SMC) (PMI 2019). The national goal for

SMC is that it be provided to all children aged 3-59 months by 2020 (PMI 2019). Currently, there are no signs of artemisinin resistance in Burkina Faso, as no molecular markers have been observed. However, recent studies suggest that first-line ACT therapies may have reduced efficacy in children aged 6-59 months (Gansané et al. 2021), and detectable parasitemia 72 hours after treatment with artemether–lumefantrine (AL) has been observed (Beshir et al. 2021).

The widespread adoption of ACTs has led to reductions in malaria prevalence in the past 10 years, but the widespread use of ACTs within Burkina Faso also places selective pressure on the parasite to evolve resistance. The impact that artemisinin-resistant *P. falciparum* would have in Burkina Faso is currently unknown; however, ensuring the continued efficacy of ACTs is a top priority for all national malaria control programs in Africa. Accordingly, the development of spatial, individual-based stochastic models allows for projections to be made as to when and where artemisinin resistant parasites may appear and how drug policies may affect the evolution of drug resistance in the parasite. In this study we have modified and calibrated a spatial individual-based model for Burkina Faso. This model has been used to explore two broad concerns: the possible emergence or importation of artemisinin resistance under the current health care regime and the impact that various drug policy interventions may have on artemisinin resistance.

Results

Baseline Configuration (de novo emergence)

A previously calibrated individual-based malaria model (Nguyen et al, 2015) was parametrized to fit mean Malaria Atlas Project *Pf*PR_{2-10} projections for Burkina Faso in 2017 on a 5km-by-5km cell (or pixel) basis (Weiss et al. 2019). Individual movement was fit to recently available travel survey data for both the destination and frequency (Fig. 1d) (Marshall et al. 2016; Marshall et al. 2018). When individuals in the model are infected, the asexual parasite density is modeled and the levels of parasitemia and immune response are used to determine symptoms occurrence and treatment seeking behavior. Individuals in the model seek treatment at different rates based upon their age group: under-5 treatment rates were based upon the Malaria Indicator Survey rates (INSD et al. 2018), while the over-5 treatment rates were adjusted to be 55% lower (relative scale) than the under-5 treatment rate to account for lower rates of treatment seeking among adults (Robyn et al. 2012). Both treatment rates are increased by 3% each model year to account for the expected increase in access to treatment over time (Bennett et al., 2017). Therapies given to individuals use a simplified single-compartment pharmacokinetic/pharmacodynamic (PK/PD) model with PK/PD parameters calibrated to reflect the expected efficacies of specific antimalarial compounds on particular *P. falciparum* genotypes (Nguyen et al. 2021), and parasitemia levels after 28 days are used to determine treatment failure.

As a baseline scenario we examined the *de novo* emergence of the *pfkelch13* 580Y allele in the context of the existing national treatments: recommended first-line therapies of AL or dihydroartemisinin-piperaquine (DHA-PPQ), artesunate (AS) or quinine for severe malaria, and private-market treatments artesunate-mefloquine (ASMQ), amodiaquine (AQ), chloroquine (CQ), and sulfadoxine-pyrimethamine (SP) (INSD et al., 2018). The model calibration and baseline status quo scenario accounted for the use of artesunate–amodiaquine (ASAQ), but post-2018 ASAQ usage was proportionally allocated to AL and DHA-PPQ usage due to the planned phase-out of ASAQ by June 2018 (PMI 2019). The *de novo* emergence rate of 580Y alleles – an unknown value in general contexts – was set using a previous model alignment exercise (Watson et al 2021); under this parameterization, 580Y alleles progress from 0.00 to 0.01 allele frequency in seven years, assuming 10% $Pf\text{PR}_{2\text{-}10}$ and 40% drug coverage with DHA-PPQ only.

Under this baseline parameterization, we found that by model year 2038 the national median frequency of 580Y would be 0.048 (IQR 0.046 – 0.052), with a treatment failure rate of 11.57% (IQR 11.52% - 11.62%), although on a local (i.e., cellular or pixel) basis the values may be higher or lower, depend strongly on the stochasticity of initial emergence (Fig. 2). Furthermore, on a provincial basis, the 580Y allele frequency reaches a median of 0.0569 (IQR 0.0512 – 0.0634); with provinces that have a high prevalence and moderate to high ACT usage at higher risk of accelerated mutation fixation. The spatial distribution of 580Y in the model confirms that (*i*) emergence is stochastic, and (*ii*) high treatment coverage coupled with either high prevalence or permanent transmission contributes to acceleration of local selection for the 580Y mutation (or another *kelch13* mutation with similar effect on artemisinin efficacy). Accordingly, the highest frequencies of 580Y under the baseline parametrization occur in the south-western Sudanian climate range (i.e., permanent transmission and high treatment coverage) and northern regions (i.e., high prevalence and high treatment coverage) of Burkina Faso.

Drug Policy Interventions

The distribution of treatments used in Burkina Faso suggests two possible drug policy interventions affecting the use of private market drugs and the deployment of nationally recommended first-line therapies. First, private-market drugs account for about 16.8% of treatments for febrile illness, with AQ monotherapy accounting for 73.8% of private-market treatments (12.4% of national treatments) (INSD et al., 2018). Reduction or elimination of private-market purchases would ensure that individuals are more likely to receive a recommended first-line therapy (always an ACT) with higher efficacy. Second, it may be possible to shift from AL as the primary single first-line therapy to the use of multiple first-line therapies (MFT) in which AL and DHA-PPQ are prescribed, distributed, and used in approximately equal amounts. The use of MFT may delay the emergence and spread of drug resistance and improve long-run clinical outcomes (Boni et al. 2008). To examine these two drug policy interventions, the baseline parametrization of current

treatment distribution was modified to include private-market elimination, MFT, or both. We investigated scenarios where immediate or gradual (phased in over ten years) implementation of MFT and private market elimination occurred (see Supplemental Table 1).

As expected, a focus solely upon the elimination of the private market results in an increase in the frequency of 580Y due to the resulting increase in ACT usage (Fig. 3). Under the rapid elimination scenario, the national median frequency of 580Y rises to 0.106 (IQR 0.010 - 0.113) by model year 2038, while under a ten-year elimination strategy median 580Y frequency in 2038 is slightly lower at 0.085 (IRQ 0.081 - 0.091). Elimination of the private market has a favorable outcome on treatment failures due to their reduction in relation to the baseline scenario, with a rapid elimination resulting in a failure rate of 8.88% (IRQ 8.80% - 8.97%) in model year 2038 and a ten-year phase out resulting in a slightly lower rate of 8.58% (IRQ 8.53% - 8.65%). This reduction in treatment failures in comparison to the baseline configuration (23% reduction for rapid elimination, and 26% reduction for ten-year phase-out), despite the higher 580Y frequency, highlights the value in ensuring that individuals use highly efficacious treatments when presenting with malaria. Note that the model predicts that the intermediate option (10-year phase-out) is the best long-term approach for reducing treatment failures, highlighting the combined effects of artemisinin-resistance evolution and high-efficacy treatment access that need to be considered in long-term drug-resistance planning.

In contrast to the elimination of the private market, the model suggests that the introduction of MFT with an equal distribution of AL and DHA-PPQ would have a negative effect on treatment failure rates due to a more rapid acceleration in 580Y frequency (Fig. 4), driven primarily by DHA-PPQ. When an MFT strategy with AL and DHA-PPQ is implemented without elimination of the private market, treatment failures increase to a national median of 21.52% (IQR 21.27% – 21.66%) by model year 2038, and 19.47% (IQR 19.31% – 19.65%) when MFT is phased in over ten years. While the frequency of 580Y is high under both scenarios, reaching a national median of 0.294 (IQR 0.283 – 0.307) by model year 2038 with rapid adoption and 0.189 (IQR 0.182 – 0.202) with a ten-year introduction, it is insufficient to account for the treatment failure rate alone suggesting multiple factors at play. The rate of treatment failures is accelerated when MFT is coupled with private market elimination. Under a rapid private market elimination scenario, coupled with the immediate adoption of MFT, the resulting national median treatment failure rate in model year 2038 of 24.92% (IQR 24.58% - 25.14%) and 580Y frequency of 0.532 (0.513 – 0.545) by the end of the simulation. This pattern of increased 580Y frequency is observed across all permutations of private market elimination and MFT adoption rates (Table 1).

This adverse MFT outcome is attributable to the increased usage of DHA-PPQ as the co-equal first-line therapy. Typically, MFT policies result in better long-term drug-resistance outcomes due to the heterogeneous drug environments they create (Boni et al. 2008; Boni et al. 2016). However, these analyses

assume that all therapies distributed in an MFT policy are equally efficacious and have identical drug-resistance properties. This is not the case when comparing DHA-PPQ and AL, as piperaquine (PPQ) resistance leads to higher levels of treatment failure when compared to lumefantrine resistance (Nguyen et al. 2021). In contrast to the baseline scenario with limited DHA-PPQ usage (5.1%), or the nominal increase resulting from private market elimination (6.2%), introduction of MFT results in DHA-PPQ usage in 46.1% of treatments when coupled with private market elimination (Supplemental Table 1). The drug policy combination of rapid private market elimination along with rapid MFT introduction results in rapid frequency increase of the *plasmepsin-2,3* double-copy genotypes conferring PPQ resistance (Witkowski et al. 2017). Effectively, following acquisition of PPQ resistance, the continued selective pressure of DHA produces an environment that is more favorable to the development of artemisinin resistance due to the lack of partner-drug killing of potentially emergent artemisinin-resistant genotypes. This is consistent with recent findings that partner-drug resistance facilitates the development of primary drug (i.e., artemisinin) resistance (Watson et al. 2021). The increased frequency of *plasmepsin-2,3* double-copy genotypes is observable shortly after implementation of the policy in model year 2021 (Fig. 5) and is present in all scenarios that implement MFT (Fig. 6).

To further investigate the parameters under which an MFT policy incorporating DHA-PPQ may be implemented in Burkina Faso, additional scenarios were considered in the absence of a private market: the use of AL as the sole first-line therapy, along with MFT combinations of AL and DHA-PPQ including a range from 60% to 90% AL use (Supplemental Table 1). When AL is used as a sole first-line therapy for uncomplicated malaria, the 580Y frequency reaches 0.115 (IQR 0.109 – 0.119) by model year 2038 with a treatment failure rate below that of the status quo scenario of 9.16% (IQR 9.09% - 9.21%). When MFT is introduced using DHA-PPQ (10% of treatments) and AL (90%) the results by model year 2038 show a small reduction in the 580Y frequency (0.111, IQR 0.103 – 0.117) and treatment failure rate (9.14%, IQR 9.04% - 9.22%) when compared to the AL as the sole first-line therapy. However, when the usage of DHA-PPQ is increased to 20% or higher, there is an increase in 580Y frequencies along with treatment failure rates by model year 2038 (Table 1, Fig.7).

Seasonal changes in alleles frequencies

As in some observed field studies (Babiker et al. 2013; Ord et al. 2007), drug-resistance allele frequencies in our model fluctuated with the periodicity of the transmission season (Supplemental Figure 13). This effect is most pronounced in regions of Burkina Faso where there is highly seasonal transmission (e.g., northern Sahelian climate zone). In order to examine this effect, additional simulations where conducted that reduced the geographic scope of the model to a single 25 sq.km cell, allowing for more model detail to be captured (see Supplementary Section 8). Our simulations show an increase in the ratio of

symptomatic/asymptomatic individuals during the rainy season, resulting in increased evolutionary pressure favoring drug resistance due to a higher proportion of *P. falciparum* infections being treated. The reason for the increase in the symptomatic/asymptomatic ratio during peak transmission likely results from several factors, namely, (*i*) a lower population-average level of immunity at the beginning of the high transmission season, (*ii*) possibility for multiple bites and repeat symptoms for individuals with low immunity, and (*iii*) correlation between low biting attractiveness and low immunity which will skew the ratio of bites on immunes/non-immunes from low to high transmission periods. Although the seasonal trend in drug-resistance frequency was up during the rainy season and down or flat during the dry season, the overall long-term trend remained upward with increasing drug resistance.

Discussion

While the evolution of drug resistance by the *P. falciparum* parasite is a pressing concern, in HBHI countries drug resistance evolution is secondary to the need to increase access to and usage of ACTs. Once access to ACTs is near universal, more attention should be turned towards the future impacts of drug resistance. As noted by Valle et al (2016), the spatial distribution of drug access and disease burden cannot be presumed to be uniform, and this heterogeneity will have onward effects on which areas need more focus on basic public health access versus drug-resistance management. As policy makers need to work within their local constraints when designing national drug policies, the overall national-scale timeline of the emergence and spread of drug resistance should still be the main focal point in the preparation and design of control strategies for drug resistance.

Presently there are early signals of ACT treatment failures starting to appear in Burkina Faso (Beshir et al. 2021; Gansané et al. 2021), although a genetic mechanism has not been identified, nor is it clear how widespread these signals are. If these signals are confirmed to have a genetic basis, then our study suggests that widespread resistance may manifest at a low level within a decade if there are no changes to drug policies. While the present drug mixture in Burkina Faso results in a low amount of evolutionary pressure on the parasite (specifically, pressure on artemisinin resistance via the 580Y allele), the rates of ACT usage are likely to increase in the future (Supplemental Section 6), indicating that evolutionary pressure will strengthen as access to ACTs increases and other interventions are implemented. Given the negative impact the private market has upon the overall treatment failure rate, policy makers may wish to explore ways to reduce or eliminate the use of private market drugs. Doing so would ensure broader use of highly efficacious ACTs and have a minimal impact upon the projected rise of drug resistance given the current drug mixture in Burkina Faso.

This study highlights the need for ACT partner-drug resistance awareness, particularly when partner-drug resistance has already been identified (Leroy et al. 2019). In the long term, drug resistance is expected

to evolve in all scenarios where population-level drug-use is sufficiently high, but resistance does not imply complete loss of efficacy. For example, in the case of lumefantrine, the efficacy of AL remains high at 89% on lumefantrine-resistant genotypes (Nguyen et al. 2021); however, DHA-PPQ efficacy drops to 77% when PPQ resistant parasites are present (Nguyen et al. 2021). Ultimately, the partner drug moderates the pace at which artemisinin resistance can emerge, rapid acquisition of resistance to the partner drug results in an acceleration of artemisinin resistance due to usage of ACT as a 'de facto monotherapy' because of low efficacy of the partner drug .

Despite the increase in drug resistance and treatment failures under a balanced MFT approach, elimination of the private market (with or without an MFT) may offer policy makers more flexibility. If MFT is not implemented, then this study suggests that the overall rate of treatment failures will go down as the public switches to more efficacious treatments. While the selective pressure on the parasite will increase, an increase in selective pressure is assumed regardless of intervention due to efforts to increase access to ACTs. Furthermore, this study suggests that the timeframe for gaining benefits from private market elimination may be quite broad. While elimination is unlikely outside of a model, phasing the private market over ten years may be achievable.

Any modeling exercise is dependent upon assumptions and simplifications that may impact the results. The primary limitation of this model is that it does not account the 2018 introduction of a broad SMC program intended to reach all children under-5 in Burkina Faso (PMI 2019). Given the recency of this broad approach to the program, limited data is available to calibrate model parameters accurately. The exclusion of SMC in our analysis likely results in a simulated prevalence that is higher than what is likely to be observed in the field. However, this needs to be moderated against the unknown impacts of the ongoing COVID-19 pandemic, which may impact malaria control programs and possibly lead to higher $Pf\text{PR}_{2\text{-}10}$ than what was used for model calibration, although the real impacts may not be quantifiable for several years (Heuschen et al. 2021; Weiss et al., 2020).

While the mutation rate used by the simulation is based upon an accepted alignment based on the observed pattern of *kelch13* evolution in SE Asia over the past two decades (Watson et al. 2021), the true mutation rate may be faster or slower. This is a common limitation of mathematical models of evolution since values for mutation parameters are difficult to estimate during short periods of observation (Carrella 2021; Willem et al. 2017). As such, the mutation rates result in simulation outputs wherein the relative results can be compared (i.e., private market elimination versus status quo) but the absolute values are susceptible to error if the mutation rate assumption is incorrect. Another limitation is the simplified nature of the pharmacokinetic model that is being used. While an individual multi-compartment model for each compounded incorporated in the simulation would be the best approach (Simpson et al. 2014), the complexity of implementation was balanced against the objectives of this simulation, namely, to ensure that

the parasite killing rate and evolutionary pressure resulting from treatment was consistent with the 24-hour timestep used by the simulation. It is not known how model misspecification of PK/PD dynamics on a minute/hour timescale affects long-term evolutionary outcome years or decades into the future.

It has been well established that asymptomatic individuals with *P. falciparum* play an important role in the propagation of the parasite between rainy seasons (Andrade et al. 2020); however, the impact that this has upon the evolution of drug resistance has not been well established. The seasonal periodicity of resistance markers that appeared in this simulation, in conjunction with previous results concerning the role that seasonality and asymptomatic carriers may play in the selection of drug-sensitive or -resistant parasites (Andrade et al. 2020; Babiker et al. 2013), suggests that more work is needed to understand how seasonal transmission affects selection. Improved simulation approaches will be necessary to assist policymakers in addressing the critical question of when ACTs will need to be replaced? While ACTs remain highly effective in Africa, this study, along with recent reports on treatment failure (Beshir et al. 2021; Gansané et al. 2021; Uwimana et al. 2020) suggest that we may be starting to enter a period of emerging artemisinin resistance and an end to the current "calm before the storm" suggested by Conrad and Rosenthal (2019). This transition is inevitable. ACT access is likely to increase in the coming years, reducing case numbers but increasing the selection pressure of artemisinin-resistant genotypes. Preparation, prevention, and preemption during this high-risk period for drug-resistance emergence will be key to ensuring that first-line treatment against *P. falciparum* continue working at high efficacy in the 2020s and 2030s.

Methods

Model Design

This study builds upon the individual-based stochastic model of malaria transmission previously developed by Nguyen et al. (2015) to incorporate space and geography. As with the initial model, individuals have attributes such as age, attractiveness to mosquitos, level of parasitemia, and so forth. In addition to the new of spatial components, the individual infection model was revised to incorporate a more realistic sporozoite challenge (see Supplemental Materials 5.1). The spatial component of the model allows for variables such as climate, heterogeneous access to treatment, and individual movement to be incorporated into the simulation.

In order to calibrate the model for Burkina Faso, we started by first preparing geographic information system (GIS) raster files for the country at the scale of 5km-by-5km pixels (or cells). These cells in turn contain the starting population of the model, approximately 3.6 million individuals or about 25% of the 2007 population of Burkina Faso, which are distributed based upon the population density of the country (WorldPop 2018). This population is allowed to grow and move throughout the simulated landscape, carrying any parasite colonies that they may be infected with as well. Data is collected from the

model starting in the simulated year 2018 which approximates the most recent Malaria Indicator Survey for Burkina Faso used for model calibration. Simulation runs using 100% versus 25% of the population size are not found to be qualitatively different.

The primary measure for artemisinin resistance in the model is the frequency of the 580Y mutation in *pfkelch13*. Upon model initialization the frequency of 580Y is zero and following the introduction of widespread ACT usage, the locus is allowed to mutate with a probability of 0.001983 per infection, where the mutation rate is based upon a model alignment exercises for the time to reach 1% allele frequency of 580Y (Watson et al. 2021). Other genetic makers associated with drug resistance here *plasmepsin-2,3* double copy, *pfmdr1* double copy, *pfcrt-k76*, *pfmdr1-N86*, *pfmdr1-184F*) are included in the model and operate in a similar fashion to 580Y with the model initialized with the sensitive genotype. For each scenario, a total of 50 replicates are performed to ensure sufficient coverage of outlier simulation results.

To evaluate the impact that various drug policies have on treatment, the simulation tracks the number of clinical cases (i.e., individuals with clinical symptoms), the reported number of cases (i.e., individuals with clinical symptoms receiving medical care), treatment failures (i.e., individuals with clinical symptoms for whom the prescribed treatment was not effective), and the number of individuals with clinical symptoms who did not seek treatment. Additionally, the genotype of the parasite, or parasites in the case of a multiclonal infection, is tracked across all individuals in the model.

Model Validation

The spatial model of Burkina Faso has 10,936 5km-by-5km (25 sq.km) pixels with a population of at least one individual at model initialization, allowing for comparisons to the annual mean *Pf*PR_{2-10} estimates for nominal year 2017, using the first data set released by the Malaria Atlas Project (Weiss et al. 2019). Each pixel is assigned a transmission parameter β which corresponds, approximately, to the local force of infection or vectorial capacity at that location. Individual pixel *Pf*PRs were calibrated by finding a β that results in the appropriate annual mean *Pf*PR_{2-10} given a cell's population size, treatment coverage, seasonal transmission pattern, and reference PfPR_{2-10}. The predicted population weighted annual mean *Pf*PR_{2-10} values for each cell were then aggregated to the province level for comparison to the Malaria Atlas Project values (Figure 1a). Individual movement was added into the model by using a modified gravity model (Zupko et al. 2021) that was re-fit from data presented in Marshall et al (2016, 2018). Pixel-level and province-level PfPR_{2-10} values were evaluated to ensure that movement did not have too large of an overall effect on PfPR_{2-10} trends. All individual movement presumes an eventual return to the original cell of the individual (i.e., round trips only), although the length of the trip is variable and may involve multiple stops. Province-level simulated PfPR_{2-10} values, with the full model (including movement), are compared to reference PfPR_{2-10} data in Figure 1. All mosquito bites in the simulation are presumed to be infectious and

the individual is infected with the parasite if they are unable to resist the initial exposure to the sporozoite (see Supplemental Information, Section 5.1).

Scenarios Comparisons

All studies evaluated use a baseline business-as-usual configuration for Burkina Faso, in which the model is parameterized to match the Malaria Atlas Project prevalence in 2017 (Weiss et al. 2019). Drug coverage (i.e., the percentage of malaria-positive febrile individuals who are able to obtain drug treatment and choose to do so) for 2017 is set to be province-specific, based on data from a 2018 malaria indicator survey (INSD et al. 2018). For symptomatic individuals that receive antimalarial treatment, the distribution of drugs used/prescribed is taken from this malaria indicator survey; however, since distribution is known only at a national level it is applied to the province-level drug coverage to get a final table of province-level treatment distributions (or lack thereof). At a national level, 16.8% of individuals use antimalarials purchased in the private market and 83.2% receive an artemisinin combination therapy in the public-sector (91.6% AL, 6.6% ASAQ, 1.8% DHA-PPQ) for uncomplicated malaria in non-pregnant individuals. To account for the phase out of ASAQ, the 6.6% was proportionally redistributed for the final business-as-usual public-sector treatment mix (93.3% AL, 6.7% DHA-PPQ). Access to treatment is assumed to go up every year in each province by about 3% starting with model year 2019 as the first year of improved access.

Building upon the business-as-usual configuration, two primary scenarios were considered: elimination of private market drugs, and introduction of MFT. These two core scenarios were then considered in the context of immediate implementation or ten-year phased implementation with adjustments to the drug distribution occurring one per model year. For private market elimination scenarios, the reduction in private market treatment usage is proportionality distributed every year to the public market treatment included in the study. Likewise, for the MFT scenario, a goal of an even distribution of AL and DHA-PPQ is assumed, and the usage of AL is reduced on an annual basis and allocated to DHA-PPQ usage until an even distribution was reached. The various permutations of private market elimination, MFT, and implementation timelines the made up eight of the thirteen drug policy scenarios examined (see Supplemental Information, Table 6). The remaining five drug policy scenarios were designed to evaluate the impact of various MFT mixes of AL and DHA-PPQ ranging from 100% AL to 50% AL by 10% reductions in AL usage. Since the intent of these scenarios is to evaluate the impact of the MFT drug mixture on the emergence of resistance, rapid private market elimination was used for all of them.

Data availability

Spatial raster files used in the simulation and long with intermediary files used for analysis and plot generation can be found at https://github.com/bonilab/malariaibm-spatial-BurkinaFaso-2021/tree/main/Data

Code availability

The source code for the base mathematical model and analysis specific to this manuscript https://github.com/bonilab/malariaibm-spatial-BurkinaFaso-2021

Acknowledgements

This work was supported by the National Institutes of Health (R01AI153355) and the Bill & Melinda Gates Foundation grants OPP159934 to the University of Washington and INV-005517 to Pennsylvania State University. Simulations described in this study were performed on the Pennsylvania State University's Institute for Computational and Data Sciences' Roar supercomputer.

Author Contributions

RJZ developed the model's spatial framework, fit the model to movement and epidemiological data, conducted the simulation studies, and drafted the manuscript. RJZ and TDN integrated the spatial framework into the previous model version and carried out epidemiological validation analyses. AFS, JG, AW, J-BO guided the calibration of the model's epidemiological and movement behaviors. TNAT parameterized the model's partial drug-resistance phenotypes and evaluated these phenotypes' trajectories in the model simulations. PD developed visualizations for model outcomes. DDHG developed a pilot model for testing. RJZ and MFB designed the simulation study and edited the manuscript. All authors read and approved the final version of the manuscript.

References

Andrade, C. M., Fleckenstein, H., Thomson-Luque, R., Doumbo, S., Lima, N. F., Anderson, C., Hibbert, J., Hopp, C. S., Tran, T. M., Li, S., Niangaly, M., Cisse, H., Doumtabe, D., Skinner, J., Sturdevant, D., Ricklefs, S., Virtaneva, K., Asghar, M., Homann, M. V., … Portugal, S. (2020). Increased circulation time of Plasmodium falciparum underlies persistent asymptomatic infection in the dry season. *Nature Medicine*, *26*(12), 1929–1940. https://doi.org/10.1038/s41591-020-1084-0

Ariey, F., Witkowski, B., Amaratunga, C., Beghain, J., Langlois, A.-C., Khim, N., Kim, S., Duru, V., Bouchier, C., Ma, L., Lim, P., Leang, R., Duong, S., Sreng, S., Suon, S., Chuor, C. M., Bout, D. M., Ménard, S., Rogers, W. O., … Ménard, D. (2014). A molecular marker of artemisinin-resistant Plasmodium falciparum malaria. *Nature*, *505*(7481), 50–55. https://doi.org/10.1038/nature12876

Ashley, E. A., Dhorda, M., Fairhurst, R. M., Amaratunga, C., Lim, P., Suon, S., Sreng, S., Anderson, J. M., Mao, S., Sam, B., Sopha, C., Chuor, C. M., Nguon, C., Sovannaroth, S., Pukrittayakamee, S., Jittamala, P., Chotivanich, K., Chutasmit, K., Suchatsoonthorn, C., … White, N. J. (2014). Spread of

Artemisinin Resistance in Plasmodium falciparum Malaria. *New England Journal of Medicine*, *371*(5), 411–423. https://doi.org/10.1056/NEJMoa1314981

Babiker, H. A., Gadalla, A. A. H., & Ranford-Cartwright, L. C. (2013). The role of asymptomatic P. falciparum parasitaemia in the evolution of antimalarial drug resistance in areas of seasonal transmission. *Drug Resistance Updates*, 16(1), 1–9. https://doi.org/10.1016/j.drup.2013.02.001

Bennett, A., Bisanzio, D., Yukich, J. O., Mappin, B., Fergus, C. A., Lynch, M., Cibulskis, R. E., Bhatt, S., Weiss, D. J., Cameron, E., Gething, P. W., & Eisele, T. P. (2017). Population coverage of artemisinin-based combination treatment in children younger than 5 years with fever and Plasmodium falciparum infection in Africa, 2003–2015: A modelling study using data from national surveys. *The Lancet Global Health*, *5*(4), e418–e427. https://doi.org/10.1016/S2214-109X(17)30076-1

Beogo, I., Huang, N., Drabo, M. K., & Yé, Y. (2016). Malaria related care-seeking-behaviour and expenditures in urban settings: A household survey in Ouagadougou, Burkina Faso. *Acta Tropica*, *160*, 78–85. https://doi.org/10.1016/j.actatropica.2016.03.033

Beshir, K. B., Diallo, N., Somé, F. A., Sombie, S., Zongo, I., Fofana, B., Traore, A., Dama, S., Bamadio, A., Traore, O. B., Coulibaly, S. A., Maurice, O. S., Diarra, A., Kaboré, J. M., Kodio, A., Togo, A. H., Dara, N., Coulibaly, M., Dao, F., … Sutherland, C. J. (n.d.). Persistent sub-microscopic Plasmodium falciparum parasitaemia 72 hours after treatment with artemether-lumefantrine predicts 42-day treatment failure in Mali and Burkina Faso. *Antimicrobial Agents and Chemotherapy*, *0*(ja), AAC.00873-21. https://doi.org/10.1128/AAC.00873-21

Boni, M. F., Smith, D. L., & Laxminarayan, R. (2008). Benefits of using multiple first-line therapies against malaria. *Proceedings of the National Academy of Sciences*, *105*(37), 14216. https://doi.org/10.1073/pnas.0804628105

Boni, M. F., White, N. J., & Baird, J. K. (2016). The Community As the Patient in Malaria-Endemic Areas: Preempting Drug Resistance with Multiple First-Line Therapies. *PLOS Medicine*, 13(3), e1001984. https://doi.org/10.1371/journal.pmed.1001984

Carrella, E. (2021). No Free Lunch when Estimating Simulation Parameters. *Journal of Artificial Societies and Social Simulation*, 24(2), 7. https://doi.org/10.18564/jasss.4572

Chenet, S. M., Akinyi Okoth, S., Huber, C. S., Chandrabose, J., Lucchi, N. W., Talundzic, E., Krishnalall, K., Ceron, N., Musset, L., Macedo de Oliveira, A., Venkatesan, M., Rahman, R., Barnwell, J. W., & Udhayakumar, V. (2015). Independent Emergence of the Plasmodium falciparum Kelch Propeller Domain Mutant Allele C580Y in Guyana. *The Journal of Infectious Diseases*, *213*(9), 1472–1475. https://doi.org/10.1093/infdis/jiv752

Conrad, M. D., & Rosenthal, P. J. (2019). Antimalarial drug resistance in Africa: The calm before the storm? *The Lancet Infectious Diseases*, *19*(10), e338–e351. https://doi.org/10.1016/S1473-3099(19)30261-0

Gansané, A., Moriarty, L. F., Ménard, D., Yerbanga, I., Ouedraogo, E., Sondo, P., Kinda, R., Tarama, C., Soulama, E., Tapsoba, M., Kangoye, D., Compaore, C. S., Badolo, O., Dao, B., Tchwenko, S., Tinto, H., & Valea, I. (2021). Anti-malarial efficacy and resistance monitoring of artemether-lumefantrine and dihydroartemisinin-piperaquine shows inadequate efficacy in children in Burkina Faso, 2017–2018. *Malaria Journal*, *20*(1), 48. https://doi.org/10.1186/s12936-021-03585-6

Heuschen, A.-K., Lu, G., Razum, O., Abdul-Mumin, A., Sankoh, O., von Seidlein, L., D'Alessandro, U., & Müller, O. (2021). Public health-relevant consequences of the COVID-19 pandemic on malaria in sub-Saharan Africa: A scoping review. *Malaria Journal*, 20(1), 339. https://doi.org/10.1186/s12936-021-03872-2

Institut National de la Statistique et de la Démographie (INSD), Programme d'Appui au Développement Sanitaire (PADS), & Programme National de Lutte contre le Paludisme (PNLP) et ICF. (2018). *Enquête sur les Indicateurs du Paludisme, 2017-2018* (pp. 1–159). https://www.dhsprogram.com/pubs/pdf/MIS32/MIS32.pdf

Leroy, D., Macintyre, F., Adoke, Y., Ouoba, S., Barry, A., Mombo-Ngoma, G., Ndong Ngomo, J. M., Varo, R., Dossou, Y., Tshefu, A. K., Duong, T. T., Phuc, B. Q., Laurijssens, B., Klopper, R., Khim, N., Legrand, E., & Ménard, D. (2019). African isolates show a high proportion of multiple copies of the Plasmodium falciparum plasmepsin-2 gene, a piperaquine resistance marker. *Malaria Journal*, *18*(1), 126. https://doi.org/10.1186/s12936-019-2756-4

Marshall, J. M., Touré, M., Ouédraogo, A. L., Ndhlovu, M., Kiware, S. S., Rezai, A., Nkhama, E., Griffin, J. T., Hollingsworth, T. D., Doumbia, S., Govella, N. J., Ferguson, N. M., & Ghani, A. C. (2016). Key traveller groups of relevance to spatial malaria transmission: A survey of movement patterns in four sub-Saharan African countries. *Malaria Journal*, *15*(1), 200. https://doi.org/10.1186/s12936-016-1252-3

Mathieu, L. C., Cox, H., Early, A. M., Mok, S., Lazrek, Y., Paquet, J.-C., Ade, M.-P., Lucchi, N. W., Grant, Q., Udhayakumar, V., Alexandre, J. S., Demar, M., Ringwald, P., Neafsey, D. E., Fidock, D. A., & Musset, L. (2020). Local emergence in Amazonia of Plasmodium falciparum k13 C580Y mutants associated with in vitro artemisinin resistance. *ELife*, *9*, e51015. https://doi.org/10.7554/eLife.51015

Ministère de la Santé. (2016). *Plan Strategique National de Lutte Contre le Paludisme 2016-2020* (pp. 1–138). Ministère de la Santé. http://onsp-sante.bf/sites/default/files/publications/166/PSN%20%20%20%20%202016-2020_Paludisme_20_02_2017.pdf

Ministère de la Santé. (2020). *État de Santé de la Population du Burkina Faso: Rapport 2019* (pp. 1–88). https://drive.google.com/uc?export=dowload&id=1K-Aw5Xp5eWH-DSd_VbGT85pi84UWptpC

Miotto, O., Sekihara, M., Tachibana, S.-I., Yamauchi, M., Pearson, R. D., Amato, R., Gonçalves, S., Mehra, S., Noviyanti, R., Marfurt, J., Auburn, S., Price, R. N., Mueller, I., Ikeda, M., Mori, T., Hirai, M., Tavul, L., Hetzel, M. W., Laman, M., … Mita, T. (2020). Emergence of artemisinin-resistant Plasmodium falciparum with kelch13 C580Y mutations on the island of New Guinea. *PLOS Pathogens*, *16*(12), e1009133. https://doi.org/10.1371/journal.ppat.1009133

Nguyen, T. D., Olliaro, P., Dondorp, A. M., Baird, J. K., Lam, H. M., Farrar, J., Thwaites, G. E., White, N. J., & Boni, M. F. (2015). Optimum population-level use of artemisinin combination therapies: A modelling study. *The Lancet Global Health*, *3*(12), e758–e766. https://doi.org/10.1016/S2214-109X(15)00162-X

Nguyen, T. D., Tran, T. N.-A., Parker, D. M., White, N. J., & Boni, M. F. (2021). Antimalarial mass drug administration in large populations and the evolution of drug resistance. *BioRxiv*, 2021.03.08.434496. https://doi.org/10.1101/2021.03.08.434496

Ord, R., Alexander, N., Dunyo, S., Hallett, R., Jawara, M., Targett, G., Drakeley, C. J., & Sutherland, C. J. (2007). Seasonal Carriage of *pfcrt* and *pfmdr1* Alleles in Gambian *Plasmodium falciparum* Imply

Reduced Fitness of Chloroquine-Resistant Parasites. *The Journal of Infectious Diseases*, 196(11), 1613–1619. https://doi.org/10.1086/522154

President's Malaria Initiative. (2019). *Burkina Faso Malaria Operational Plan FY 2019* (pp. 1–51). https://www.pmi.gov/docs/default-source/default-document-library/malaria-operational-plans/fy19/fy-2019-burkina-faso-malaria-operational-plan.pdf?sfvrsn=3

President's Malaria Initiative. (2020). *Burkina Faso Malaria Operational Plan FY 2020* (pp. 1–88). https://www.pmi.gov/docs/default-source/default-document-library/malaria-operational-plans/fy20/fy-2020-burkina-faso-malaria-operational-plan.pdf

Simpson, J. A., Zaloumis, S., DeLivera, A. M., Price, R. N., & McCaw, J. M. (2014). Making the Most of Clinical Data: Reviewing the Role of Pharmacokinetic-Pharmacodynamic Models of Anti-malarial Drugs. *The AAPS Journal*, *16*(5), 962–974. https://doi.org/10.1208/s12248-014-9647-y

Uwimana, A., Legrand, E., Stokes, B. H., Ndikumana, J.-L. M., Warsame, M., Umulisa, N., Ngamije, D., Munyaneza, T., Mazarati, J.-B., Munguti, K., Campagne, P., Criscuolo, A., Ariey, F., Murindahabi, M., Ringwald, P., Fidock, D. A., Mbituyumuremyi, A., & Menard, D. (2020). Emergence and clonal expansion of in vitro artemisinin-resistant Plasmodium falciparum kelch13 R561H mutant parasites in Rwanda. *Nature Medicine*. https://doi.org/10.1038/s41591-020-1005-2

Valle, D., Millar, J., & Amratia, P. (2016). Spatial heterogeneity can undermine the effectiveness of country-wide test and treat policy for malaria: A case study from Burkina Faso. *Malaria Journal*, *15*(1), 513. https://doi.org/10.1186/s12936-016-1565-2

Watson, O. J., Gao, B., Nguyen, T. D., Tran, T. N.-A., Penny, M. A., Smith, D. L., Okell, L., Aguas, R., & Boni, M. F. (2021). Pre-existing partner-drug resistance facilitates the emergence and spread of artemisinin resistance: A consensus modelling study. *BioRxiv*, 2021.04.08.437876. https://doi.org/10.1101/2021.04.08.437876

Weiss, D. J., Bertozzi-Villa, A., Rumisha, S. F., Amratia, P., Arambepola, R., Battle, K. E., Cameron, E., Chestnutt, E., Gibson, H. S., Harris, J., Keddie, S., Millar, J. J., Rozier, J., Symons, T. L., Vargas-Ruiz, C., Hay, S. I., Smith, D. L., Alonso, P. L., Noor, A. M., … Gething, P. W. (2020). Indirect effects of the COVID-19 pandemic on malaria intervention coverage, morbidity, and mortality in Africa: A geospatial modelling analysis. *The Lancet Infectious Diseases*. https://doi.org/10.1016/S1473-3099(20)30700-3

Weiss, D. J., Lucas, T. C. D., Nguyen, M., Nandi, A. K., Bisanzio, D., Battle, K. E., Cameron, E., Twohig, K. A., Pfeffer, D. A., Rozier, J. A., Gibson, H. S., Rao, P. C., Casey, D., Bertozzi-Villa, A., Collins, E. L., Dalrymple, U., Gray, N., Harris, J. R., Howes, R. E., … Gething, P. W. (2019). Mapping the global prevalence, incidence, and mortality of Plasmodium falciparum, 2000–17: A spatial and temporal modelling study. *The Lancet*, *394*(10195), 322–331. https://doi.org/10.1016/S0140-6736(19)31097-9

Whitty, C. J., Chandler, C., Ansah, E., Leslie, T., & Staedke, S. G. (2008). Deployment of ACT antimalarials for treatment of malaria: Challenges and opportunities. *Malaria Journal*, *7*(1), S7. https://doi.org/10.1186/1475-2875-7-S1-S7

Willem, L., Verelst, F., Bilcke, J., Hens, N., & Beutels, P. (2017). Lessons from a decade of individual-based models for infectious disease transmission: A systematic review (2006-2015). *BMC Infectious Diseases*, 17(1), 612. https://doi.org/10.1186/s12879-017-2699-8

538 Witkowski, B., Duru, V., Khim, N., Ross, L. S., Saintpierre, B., Beghain, J., Chy, S., Kim, S., Ke, S., Kloeung,
539 N., Eam, R., Khean, C., Ken, M., Loch, K., Bouillon, A., Domergue, A., Ma, L., Bouchier, C., Leang, R.,
540 … Ménard, D. (2017). A surrogate marker of piperaquine-resistant Plasmodium falciparum malaria:
541 A phenotype–genotype association study. *The Lancet Infectious Diseases*, *17*(2), 174–183.
542 https://doi.org/10.1016/S1473-3099(16)30415-7

543 World Health Organization. (2019a). *World Malaria Report 2019* (ISBN: 978-92-4-156572-1; pp. 1–232).
544 World Health Organization. https://www.who.int/publications/i/item/world-malaria-report-2019

545 World Health Organization. (2019b). *Artemisinin resistance and artemisinin-based combination therapy*
546 *efficacy* (pp. 1–6) [Status Report]. World Health Organization. https://www.who.int/docs/default-
547 source/documents/publications/gmp/who-cds-gmp-2019-17-eng.pdf

548 WorldPop. (2018). *Global High Resolution Population Denominators Project* [Map].
549 https://dx.doi.org/10.5258/SOTON/WP00645

550 Zupko, R., Nguyen, T. D., & Boni, M. F. (2021, September 20). Simulating Human Movement in a National-
551 Scale Individual-Based Model of Malaria in Burkina Faso. *Social Simulation Conference 2021*, Kraków,
552 Poland. https://mol.ax/pdf/zupko21.pdf

553

554 **Figures**

555 **Fig. 1: Model calibration and validation.** (**a**) The first point of validation for the model is the comparison
556 of the simulated *Pf*PR$_{2\text{-}10}$ values versus the reference *Pf*PR$_{2\text{-}10}$ values from the Malaria Atlas Project (Weiss
557 et al. 2019). The annual mean of the simulated *Pf*PR$_{2\text{-}10}$ values (light gray dots) are plotted along the y-axis
558 while the reference *Pf*PR$_{2\text{ to }10}$ is plotted along the x-axis and the closer to agreement (i.e., dashed line) the
559 better. The upper and lower dark gray dots indicate the annual peak and minimum of the seasonal *Pf*PR$_{2\text{-}10}$
560 for the given province. **(b)** Clinical (i.e., symptomatic) cases of malaria plotted against the *Pf*PR$_{2\text{-}10}$, for
561 every province. Black dots correspond to every clinical case in the simulation, while gray dots are the
562 clinical cases that would be reported (according to drug coverage numbers). (**c**) The treatment seeking rate
563 used to inform the model is dependent upon the region of Burkina Faso that an individual is in, with the
564 under-5 treatment rate ranging from a low of 52.1% to a high of 87.0%. Note that the over-5 treatment
565 seeking rate is adjusted to be 45% of the under-5 treatment seeking rate to account for the lower treatment
566 seeking rate in the older demographic. (**d**) A second point of validation for the model is ensuring that
567 movement is consistent with expected patterns. Heatmap shows the number of trips to the destination cell
568 over the course of a single month in the model. Note that the distribution indicates that while there is always
569 a low chance that an individual may visit any cell, individuals are primarily attracted to major population
570 centers. Subfigure (c) reproduced from Zupko et al. (2021).

571

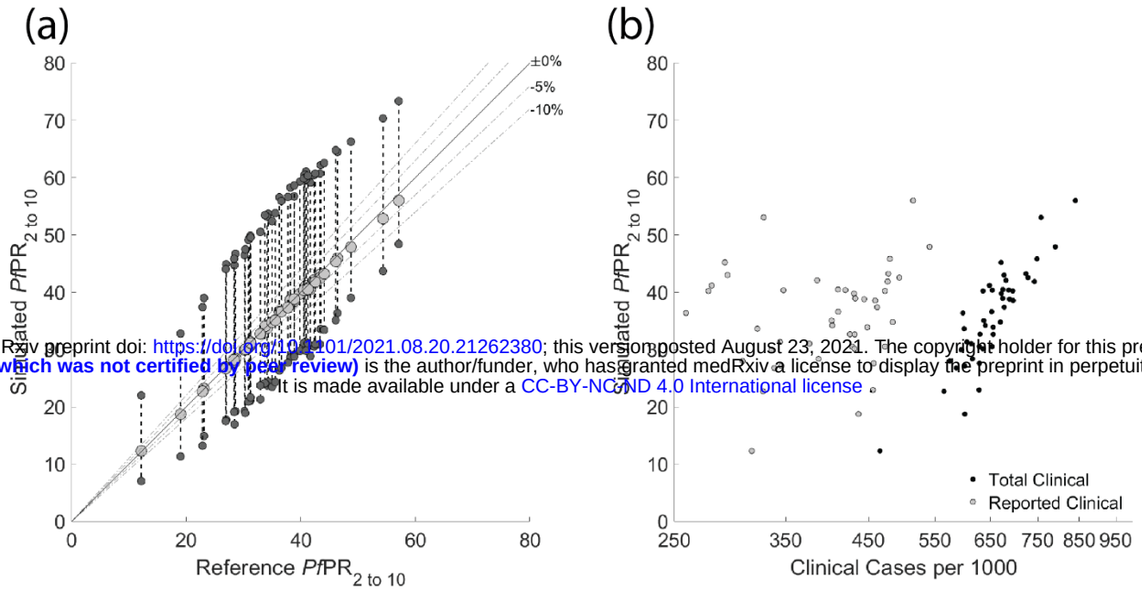

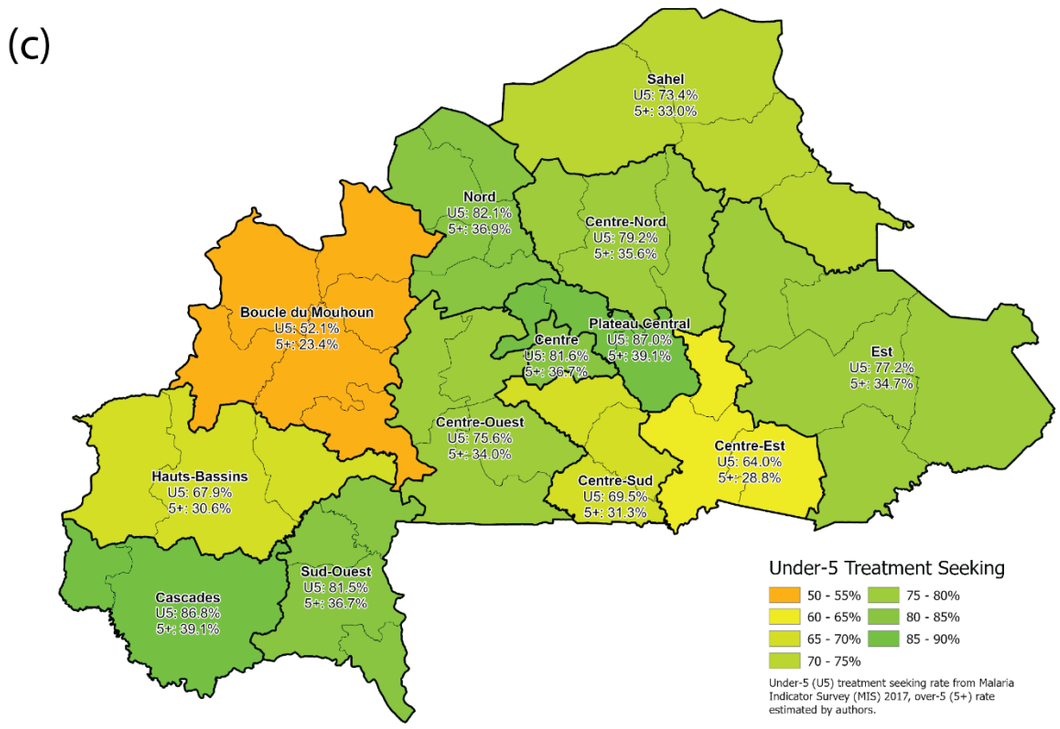

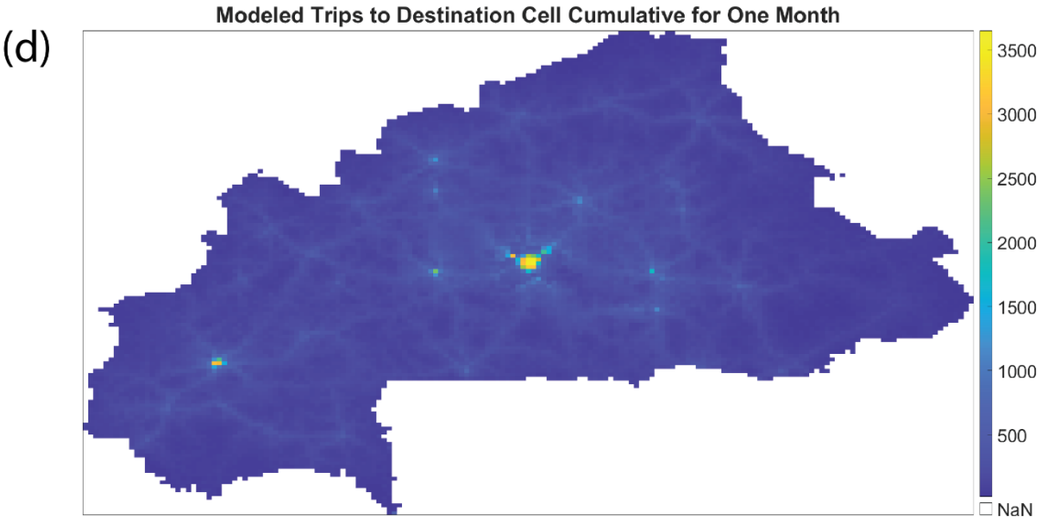

572

573

Fig. 2: *De novo* emergence of artemisinin resistance under the baseline, status quo scenario. In the first baseline scenario, C580 is allowed to mutate into 580Y using a mutation rate that has been fit to a previously calibrated pattern of artemisinin resistance in the presence of widespread ACT usage. While the emergence of artemisinin resistance in model year 2021 appears to be stochastic with only minimal evidence of the mutation in the eastern part of the country, by model year 2036 the highest frequencies of artemisinin resistance correspond to areas with persistent transmission and high access to treatment.

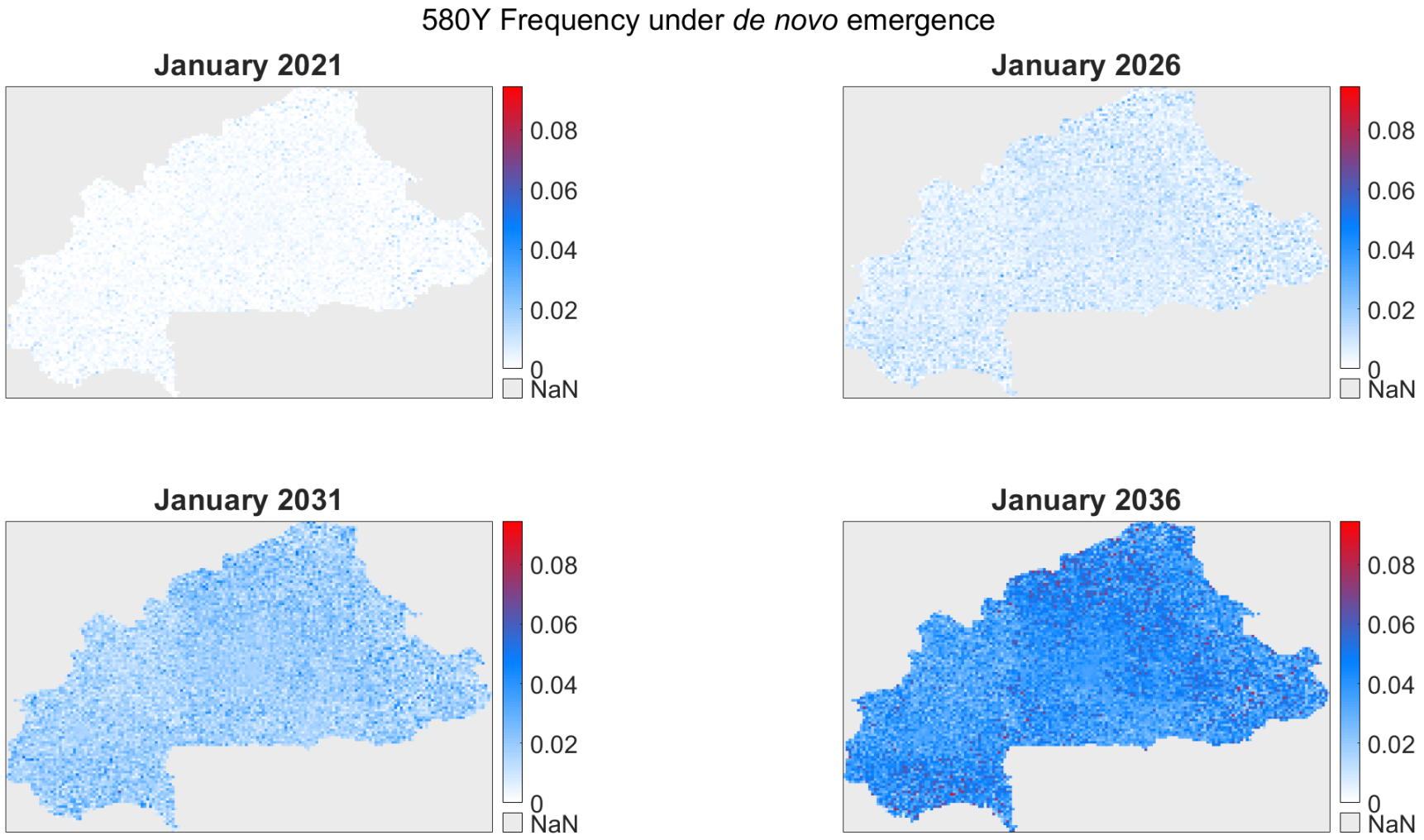

580 **Fig. 3: Comparison of 580Y frequency under various drug policy scenarios.** As expected, increased
581 use of ACTs due to private market elimination results in an increase in the frequency of 580Y under all
582 drug policies. Implementation of MFT results in higher long-term 580Y frequencies due to the high failure
583 rate of PPQ-resistant parasites.

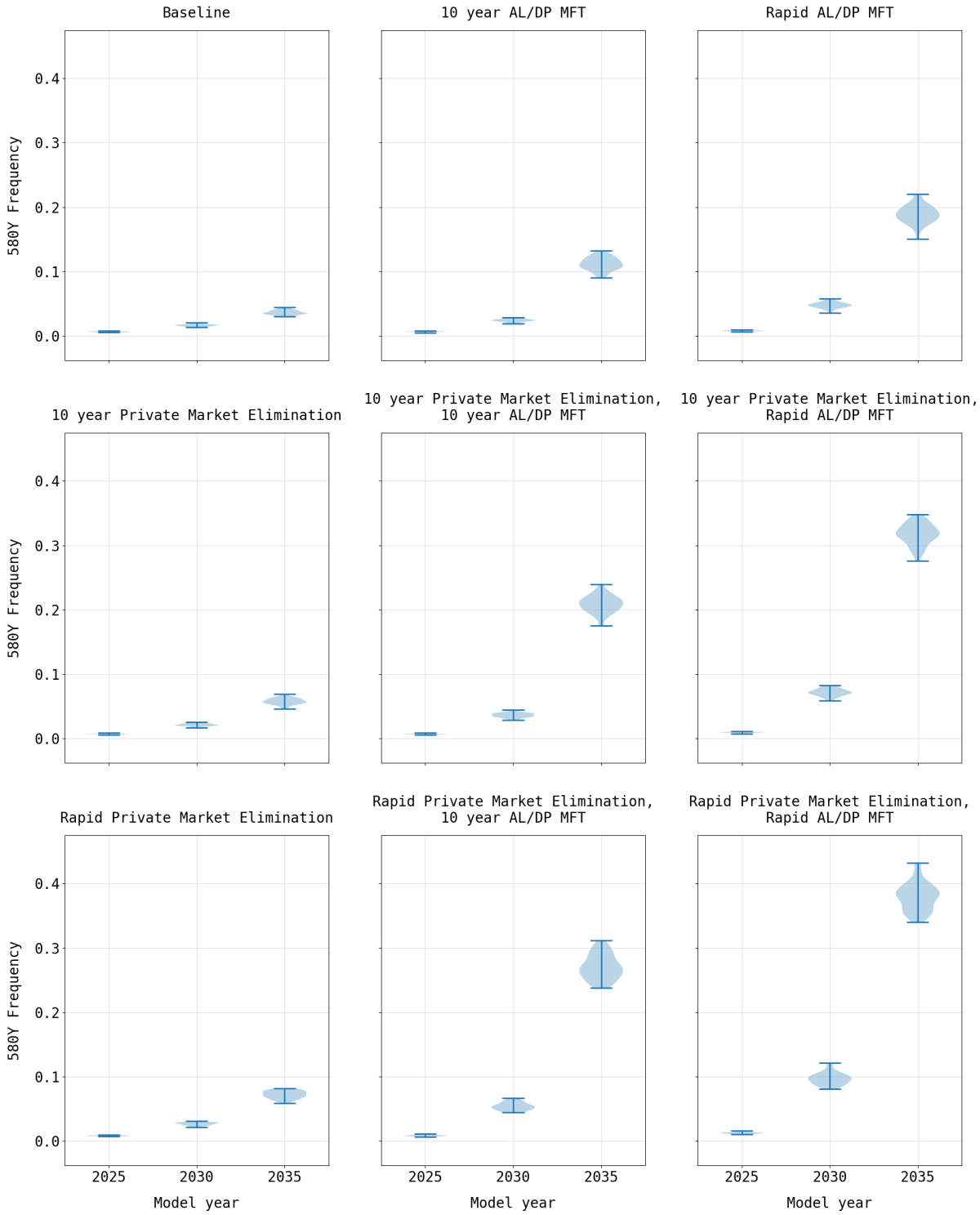

584

585 **Fig. 4: Comparison of treatment failure rates under various policy scenarios.** Under the baseline
586 scenario the treatment failure rate remains fairly consistent year to year. With elimination of the private
587 market, the treatment failure rate drops, which is expected given the elimination of less efficacious
588 treatments. Introduction of MFT plus elimination of the private market has a similar positive outcome;
589 however, this is rapidly offset by the increased treatment failure rate due to the increasing frequency of
590 *plasmepsin-2,3* double-copy genotypes.

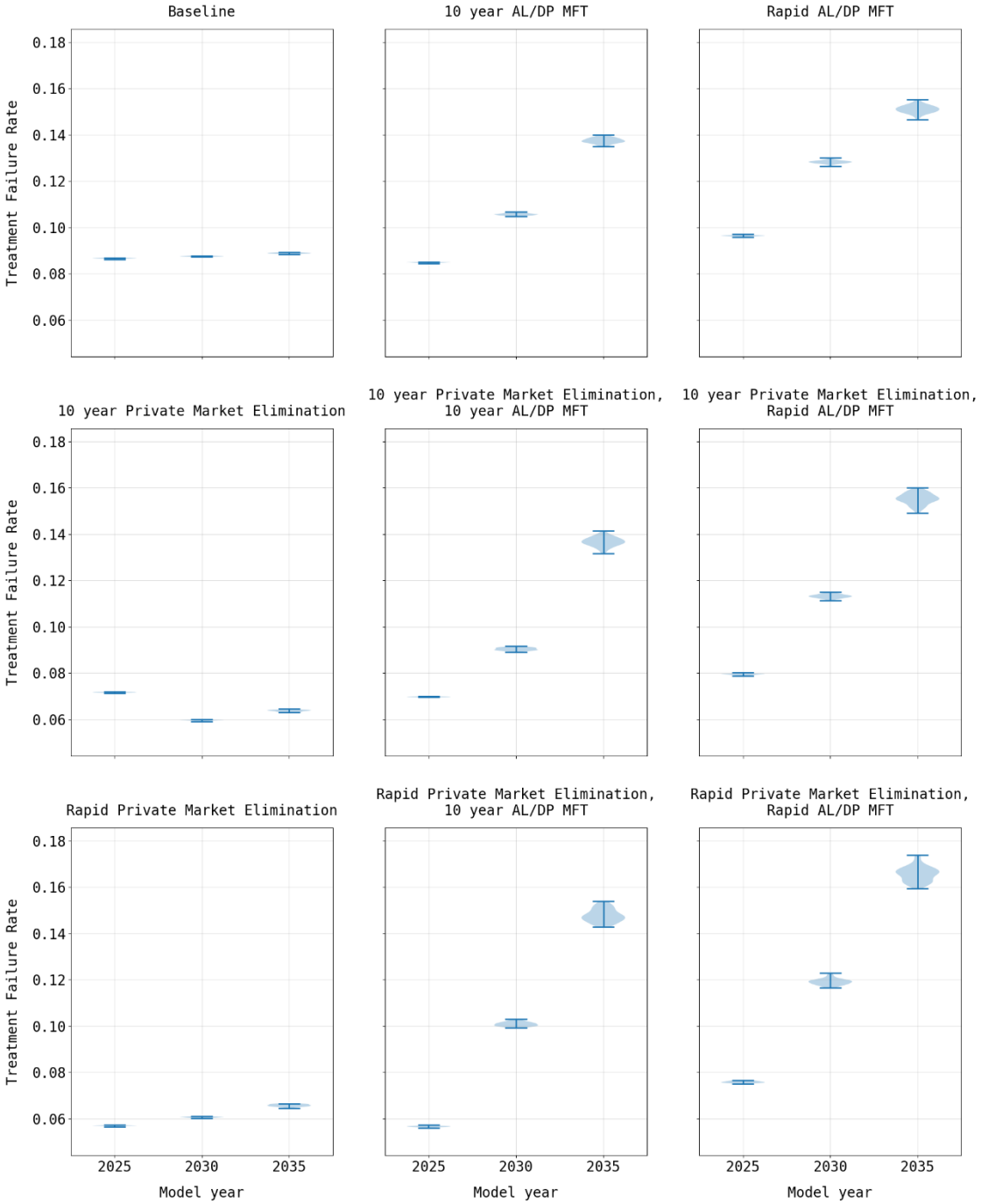

591

Fig. 5: Increase of *plasmepsin-2,3* double-copy genotypes under immediate private-market elimination and immediate MFT. The rapid elimination of the private market coupled with introduction of MFT (in model year 2021) serves as an exemplar of the rapid increase in double-copy *plasmepsin-2,3* genotypes after DHA-PPQ is introduced at high levels in 2021. Double-copy *plasmepsin-2,3* genotypes (blue) are strongly selected for after DHA-PPQ is introduced, which contrasts with the slower pace of 580Y evolution (orange). This rapid increase in the frequency of the double-copy *plasmepsin-2,3* genotypes result from the low efficacy of DHA-PPQ on these genotypes (77% efficacy on C580 and 42% on 580Y). KNF genotypes (green) show the most resistance to lumefantrine, but the efficacy of AL on a KNF genotypes is 89% (C580) or 72% (580Y) making the selection pressure exerted by AL weaker than the selection pressure exerted by DHA-PPQ.

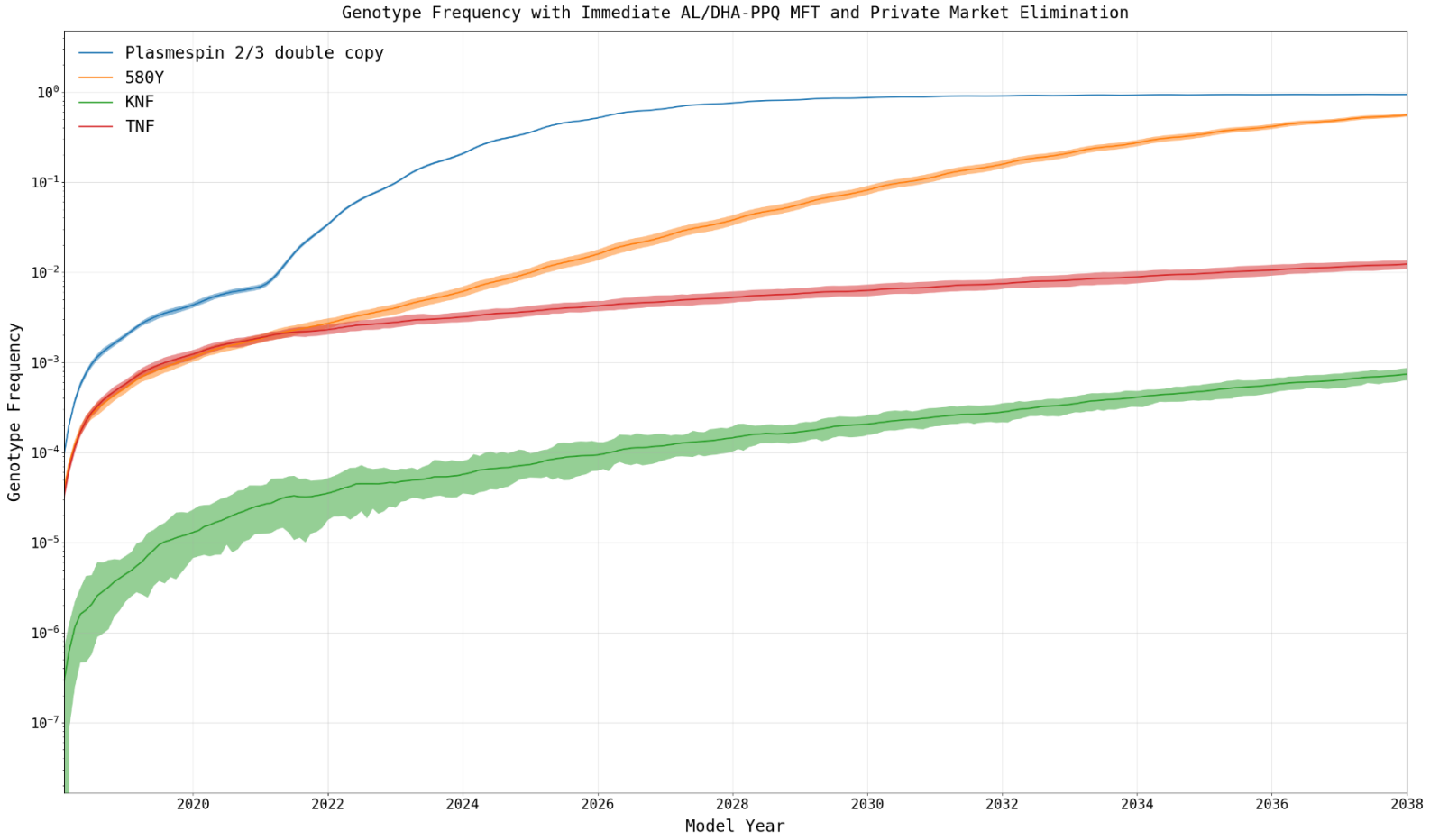

Fig. 6: Comparison of *plasmepsin-2,3* double-copy frequency under various drug policies. Under policies of private market elimination, there is little effect on DHA-PPQ usage and thus low pressure on *plasmepsin-2,3* evolution. When MFT is introduced, the usage of DHA-PPQ increases substantially, resulting in rapid selection of double-copy *plasmepsin-2,3* genotypes.

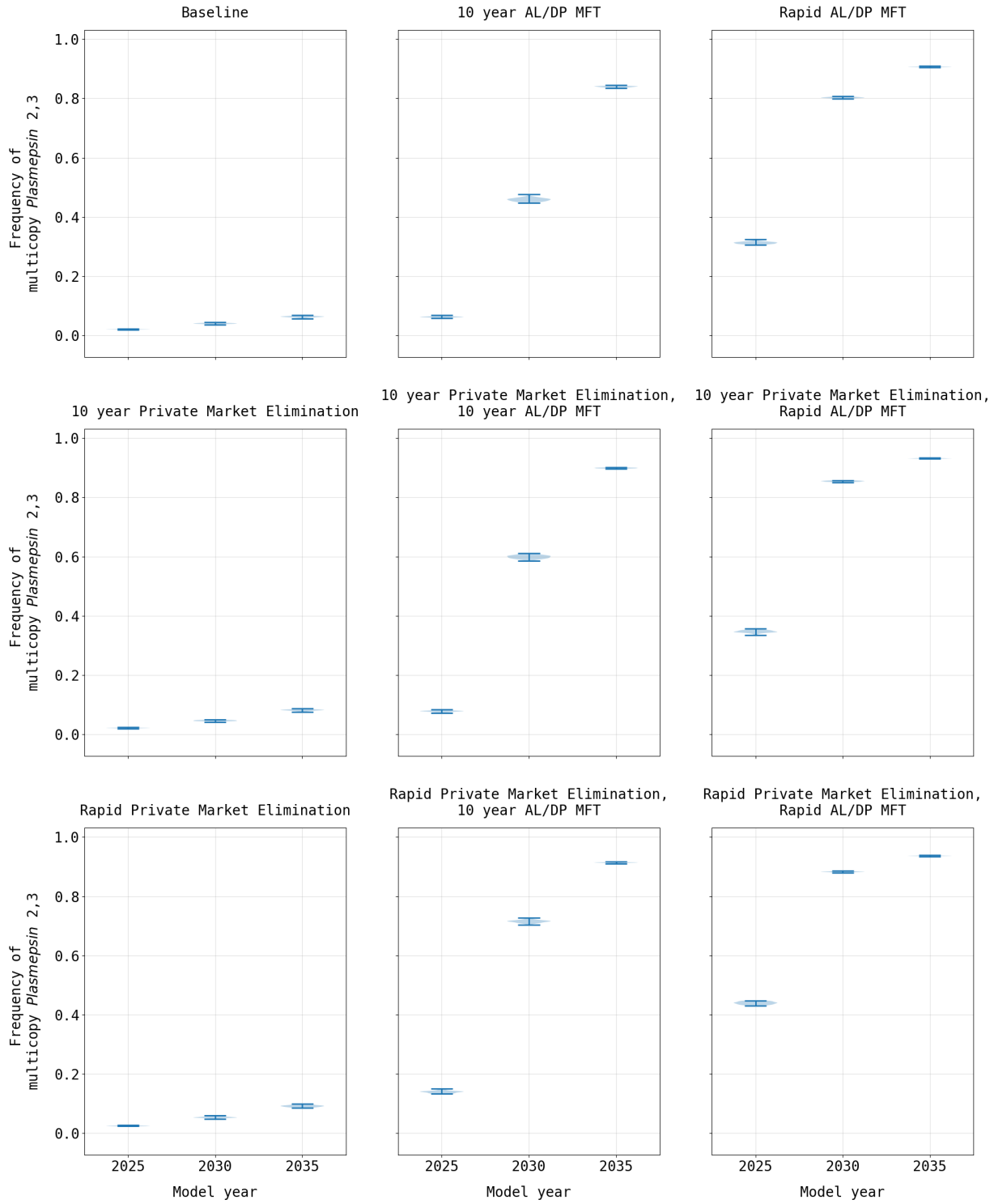

Fig. 7: 580Y frequency under various MFT configurations. The impact of changing the role of DHA-PPQ in an MFT policy. Lower DHA-PPQ use results in weaker selection pressure on 580Y alleles. The loss of PPQ efficacy due to *plasmepsin-2,3* double-copy emergence is correlated with the rate at which the 580Y frequency increases.

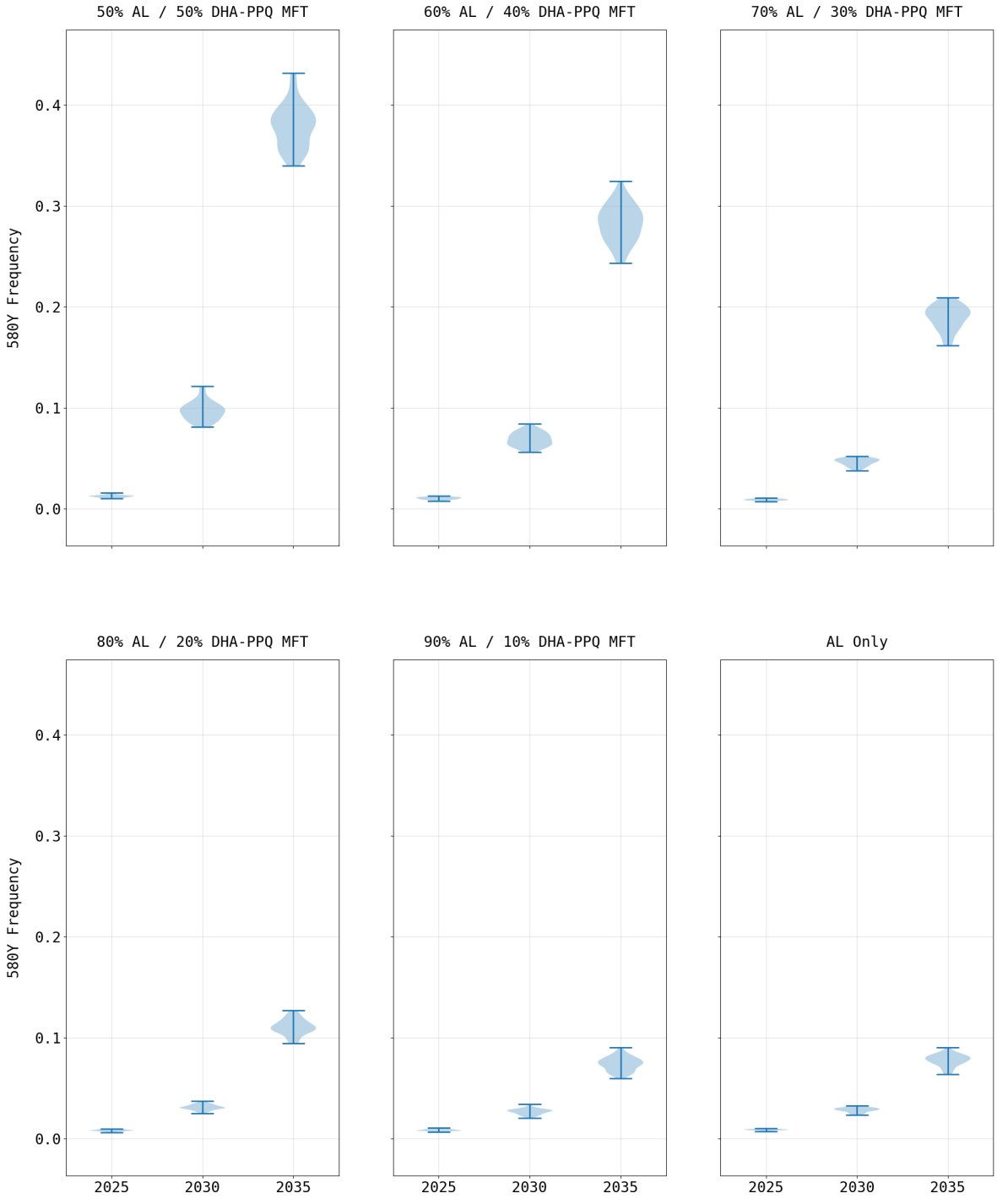

Table 1. Drug policies examined in this study. Note that all policy interventions result in a higher 580Y frequency compared to the status quo scenario, but this may be offset by reductions in the treatment failure rate for some policies. Note that the MFT scenarios assume rapid private market (PM) elimination and that unless otherwise specified the MFT is 50% AL and 50% DHA-PPQ.

Drug Policy Studies	580Y Frequency		Treatment Failure Rate	
	Median	IQR	Median	IQR
Status Quo	0.048	0.046 - 0.052	11.57%	11.52% - 11.62%
Rapid AL/DPA-PPQ MFT	0.294	0.283 - 0.307	21.52%	21.27% - 21.66%
Rapid AL/DPA-PPQ MFT, Rapid PM Elimination	0.532	0.513 - 0.545	24.92%	24.58% - 25.14%
Rapid AL/DPA-PPQ MFT, 10 Year PM Elimination	0.471	0.463 - 0.484	23.61%	23.40% - 23.83%
10 Year AL/DPA-PPQ MFT	0.189	0.182 - 0.202	19.47%	19.31% - 19.65%
10 Year AL/DPA-PPQ MFT, Rapid PM Elimination	0.420	0.407 - 0.439	22.62%	22.34% - 22.99%
10 Year AL/DPA-PPQ MFT, 10 Year PM Elimination	0.350	0.340 - 0.362	21.05%	20.82% - 21.25%
Rapid PM Elimination	0.106	0.010 - 0.113	8.88%	8.80% - 8.97%
10 Year PM Elimination	0.085	0.081 - 0.091	8.58%	8.53% - 8.65%
MFT (60% AL, 40% DPA-PPQ)	0.425	0.407 - 0.434	20.46%	20.16% - 20.70%
MFT (70% AL, 30% DPA-PPQ)	0.302	0.288 - 0.311	16.13%	15.93% - 16.27%
MFT (80% AL, 20% DPA-PPQ)	0.178	0.172 - 0.184	12.01%	11.91% - 12.10%
MFT (90% AL, 10% DPA-PPQ)	0.111	0.103 - 0.117	9.14%	9.04% - 9.22%
AL Only, Rapid PM Elimination	0.115	0.109 - 0.119	9.16%	9.09% - 9.21%